Provided for non-commercial research and education use.
Not for reproduction, distribution or commercial use.

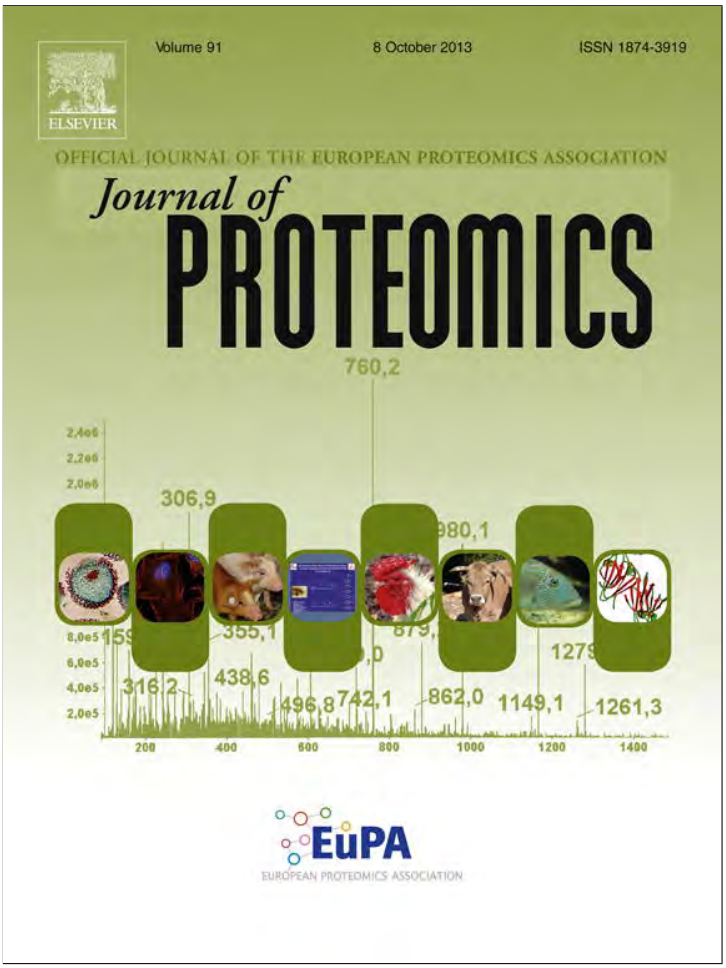

This article appeared in a journal published by Elsevier. The attached copy is furnished to the author for internal non-commercial research and education use, including for instruction at the authors institution and sharing with colleagues.

Other uses, including reproduction and distribution, or selling or licensing copies, or posting to personal, institutional or third party websites are prohibited.

In most cases authors are permitted to post their version of the article (e.g. in Word or Tex form) to their personal website or institutional repository. Authors requiring further information regarding Elsevier's archiving and manuscript policies are encouraged to visit:

http://www.elsevier.com/authorsrights

Author's personal copy

JOURNAL OF PROTEOMICS 91 (2013) 41–57

Available online at www.sciencedirect.com

ScienceDirect

www.elsevier.com/locate/jprot

Signaling proteins in spinal parenchyma and dorsal root ganglion in rat with spinal injury-induced spasticity

Helena Kupcova Skalnikova[a], *Roman Navarro*[b], *Silvia Marsala*[b], *Rita Hrabakova*[a], *Petr Vodicka*[c,d], *Suresh Jivan Gadher*[e], *Hana Kovarova*[a,*], *Martin Marsala*[b,f]

[a]*Institute of Animal Physiology and Genetics, Academy of Sciences of the Czech Republic, v.v.i., Laboratory of Biochemistry and Molecular Biology of Germ Cells, Libechov, Czech Republic*
[b]*University of California San Diego, Department of Anesthesiology, San Diego, CA, USA*
[c]*Institute of Animal Physiology and Genetics, Academy of Sciences of the Czech Republic, v.v.i., Laboratory of Cell Regeneration and Plasticity, Libechov, Czech Republic*
[d]*Massachusetts General Hospital, Department of Neurology, Boston, MA, USA*
[e]*Life Technologies, Frederick, MD, USA*
[f]*Institute of Neurobiology, Slovak Academy of Sciences, Kosice, Slovak Republic*

ARTICLE INFO

Article history:
Received 27 March 2013
Accepted 28 June 2013
Available online 5 July 2013

Keywords:
Spinal cord trauma
Spasticity
Hyper-reflexia
Proteomic profiling
Dorsal root ganglia
Spinal gray matter

ABSTRACT

Development of progressive muscle spasticity resulting from spinal traumatic injury can be mediated by loss of local segmental inhibition and/or by an increased sensory afferent drive with resulting exacerbated α-motoneuron activity. To identify potential contributions of neuroactive substances in the development of such spasticity state, we employed a well-defined spinal injury-evoked spasticity rat model. Signaling molecules were analyzed in the spinal parenchyma below the level of spinal injury and in the corresponding dorsal root ganglion cells using Kinex™ antibody microarrays. The results uncovered the involvement of angiogenesis and neurodegeneration pathways together with direct cross-talk mediated by several hub proteins with SH-2 domains. At 2 and 5 weeks after transection, up-regulation of several proteins including CaMKIV, RONα and PKCδ as well as MAPK3/ERK1 phosphorylation was observed in the spinal ventral horns. Our results indicate that these signaling molecules and their neuronal effector systems cannot only play an important role in the initiation but also in the maintenance of spasticity states after spinal trauma. The exclusivity of specific protein changes observed in lumbar spinal parenchyma but not in dorsal root ganglia indicates that new treatment strategies should primarily target specific spinal segments to prevent or attenuate spasticity states.

Abbreviations: AMPA, α-amino-3-hydroxy-5-methyl-4-isoxazolepropionic acid; CaMK, calcium/calmodulin-dependent protein-serine kinase; CASP, pro-caspase; CK, casein protein-serine kinase; CREB, cAMP response element binding protein; DRG, dorsal root ganglion; eIF4G, eukaryotic translation initiation factor 4 gamma; EMG, electromyography; eNOS, endothelial nitric oxide synthase; ERK, extracellular signal-regulated kinase; FAK, focal adhesion protein-tyrosine kinase; FGFR, fibroblast growth factor receptor; GABA, gamma-aminobutyric acid; I2D, interologous interaction database; IGFR, insulin-like growth factor receptor; iNOS, inducible nitric oxide synthase; JNK, c-Jun N-terminal kinase; Lck, lymphocyte-specific protein-tyrosine kinase; LTP, long-term potentiation; MAPK, mitogen-activated protein kinase; MEKK4, MAPK/ERK kinase kinase 4; MSP, macrophage-stimulating protein; NMDA, *N*-methyl D-aspartate; PK, protein kinase; RONα, macrophage-stimulating protein receptor alpha chain; SCI, spinal cord injury; TEK/TIE2, angiopoietin-1 receptor-tyrosine kinase; VEGFR, vascular endothelial growth factor receptor

* *Corresponding author*. Tel.: +420 315 639 582; fax: +420 315 639 510.
E-mail address: kovarova@iapg.cas.cz (H. Kovarova).

1874-3919/$ – see front matter © 2013 Elsevier B.V. All rights reserved.
http://dx.doi.org/10.1016/j.jprot.2013.06.028

Author's personal copy

Biological significance

Development of progressive muscle spasticity and rigidity represents a serious complication associated with spinal ischemic or traumatic injury. Signaling proteins, including their phosphorylation status, were analyzed in the spinal parenchyma below the level of spinal injury and in the corresponding dorsal root ganglion cells in a rat model of spinal injury using Kinex™ antibody microarrays. The results uncovered direct protein interaction mediated cross-talk between angiogenesis and neurodegeneration pathways, which may significantly contribute to the healing process in the damaged region. Importantly, we identified several target proteins exclusively observed in the spinal lumbar ventral horns, where such proteins may not only play an important role in the initiation but also in the maintenance of spasticity states after spinal trauma. Hence, potential new treatment strategies such as gene silencing or drug treatment should primarily target spinal parenchymal sites at and around the injury epicenter and most likely employ intrathecal or targeted spinal segment-specific vector or drug delivery. We believe that this work will stimulate future translational research, ultimately leading to the improvement of quality of life of patients with spinal traumatic injury.

© 2013 Elsevier B.V. All rights reserved.

1. Introduction

Development of progressive muscle spasticity and rigidity represents serious complications associated with spinal ischemic or traumatic injury. Spasticity is defined as velocity-dependent increase in muscle tone described as progressive increase in muscle resistance with increased velocity of muscle stretch; whereas rigidity is characterized by the presence of velocity-independent increase in muscle tone [1,2]. According to the National Spinal Cord Injury Statistical Center, there are approximately 12,000 new cases of spinal cord injury (SCI) every year in the United States (https://www.nscisc.uab.edu/) and 130,000 new injuries are reported annually worldwide [3]. Systematic clinical studies show that 36–80% of patients with spinal traumatic injury show gradual appearance of muscle spasticity or rigidity several months to years after spinal trauma [4–6]. The underlying mechanism leading to a progressive appearance of clinically defined spasticity is multifactorial and may include the loss of descending motor tracts as well as other modulatory pathways that control the activity of spinal inhibitory circuits. Resultant loss of descending inhibition has been linked with: i) increase in tonic α-motoneuron firing [7,8], ii) increase in Ia afferent-mediated input during muscle stretch [9], and/or iii) exacerbated sensory responses to peripheral c-fiber stimulation known as allodynia [10,11]. Loss or decrease in gamma-aminobutyric acid (GABA)-mediated presynaptic [12], recurrent [13] and reciprocal [14] inhibition as well as the loss of its inhibitory effect in flexor afferent pathway [15] has been shown to represent one of the key mechanisms leading to the development of these neurologically and electrophysiologically defined pathological states [5]. Consistent with the role of altered inhibition in the evolution of chronic spasticity, pharmacological and clinical experimental studies have demonstrated a potent anti-spasticity effect after systemic or intrathecal delivery of baclofen (GABA B receptor agonist) [16], systemic treatment with tizanidine (α2-adrenergic agonist) [17], or dorsal rhyzotomy [18]. With reference to previous studies and using rat model of chronic spinal ischemia-induced spasticity and rigidity, we have demonstrated a comparable anti-spasticity effect after intrathecal treatment with nipecotic acid (GABA uptake inhibitor) or baclofen [9], and α-amino-3-hydroxy-5-methyl-4-isoxazolepropionic acid (AMPA) receptor antagonist NGX424 in spastic baclofen non-treated [19] or spastic baclofen-tolerant animals [20].

In addition to a well-documented role of an altered GABA system in spasticity, several other neuromodulators/signaling molecules have been shown to participate in potentiating neuronal activity under a variety of pathological conditions. It has been demonstrated that proinflammatory cytokines TNF-α, IL-1β, and IL-6 or chemokines CCL2/MCP-1 and CX3CL1/fractalkine as well as growth factors released by spinal glial cells maintain the neuropathic pain after nerve injury or inflammation [21]. Nerve injury or spinal cord injury induces a profound activation of mitogen-activated protein kinases (MAPKs) in glial cells and neurons in the spinal cord. The three sub-groups of MAPKs, namely extracellular signal regulated kinases (ERKs), p38 MAPK and c-Jun N-terminal kinases (JNKs) are activated in spinal glia after nerve injury and play an important role in chronic pain sensitization by signaling to the inflammatory mediators [21]. High levels of ERK activation following SCI were correlated with increased expression of the neurokinin-1 receptor, *N*-methyl D-aspartate (NMDA) receptor subunits NR1, NR2A and the transcription factor cAMP response element binding protein (CREB) [22]. Glutamate transmission via NMDA inclusive of AMPA/kainate receptors is essential for ERK activation in spinal cord dorsal horn neurons [23] as well as α-motoneurons [18]. Additionally, potentiation of extracellular calcium influx into nociceptive neurons after glutamate receptor activation has been demonstrated to be linked to increased activity of multiple intracellular protein kinases including calcium/calmodulin-dependent protein-serine kinase 2 (CaMKII), protein kinase A and C (PKA and PKC). PKC is widely reported to play a role in long term potentiation of spinal nociceptive neurons [24,25]. The role of several such signaling molecules in the development of spasticity remains to be defined.

In recent years, several molecular–analytical techniques have been used to characterize changes in spinal parenchyma mainly during early acute and sub-acute stages after SCI. cDNA microarrays were used to characterize global changes in gene transcripts following SCI [26,27]. Two-dimensional gel

Author's personal copy

electrophoresis was commonly used to identify changes at protein levels [28–32]. However, recent advances in proteomics offer new approaches including quantitative mass spectrometry and protein arrays, where mass spectrometry is the key technology contributing to the proteome studies including phosphoproteomes. Such protein phosphorylation studies require a lot of starting material and phospho-peptide enrichment [33]. On the other hand, antibody-dependent protein arrays facilitate in depth studies of cell signaling proteins and their regulatory phosphorylations using low μg amount of cell lysate proteins. Regardless of the proteomic approaches to date, molecular changes that might contribute to secondary damage and thus increase functional deficits including appearance of spasticity after SCI have not been satisfactorily characterized. Additionally, no conclusive data is available at present that would provide a temporal and spatial characterization of the protein changes analyzed in parallel in spinal parenchyma and dorsal root ganglion cells (DRGs) at time points corresponding to the secondary damage and development of spinal trauma-induced spasticity.

In the present study, by using rat spinal transection model of chronic spasticity coupled with Kinex™ antibody microarrays, we have characterized the levels as well as phosphorylation status of a large number of signaling proteins, including kinases, phosphatases and other proteins, which were simultaneously analyzed in each of the samples of lumbar spinal gray matter or DRGs caudal to the spinal injury site. The data obtained was statistically analyzed for differences between spinal transection and control samples and additionally, further evaluated using bioinformatic tools, thus allowing implementation of regulated proteins into cellular signaling and protein interaction networks. Selected significant quantitative changes in protein levels/phosphorylations were verified using western blot and localization of these proteins within specific neural cell types was confirmed by immunofluorescence staining and confocal microscopy.

2. Material and methods

All procedures were approved by the Institutional Animal Care Committee at the University of California, San Diego (Protocol No. S01193) and were in compliance with The Association for Assessment of Laboratory Animal Care guidelines for Animal use. All efforts were made to minimize group size with respect to statistical study evaluation as well as animal suffering. Male Sprague–Dawley rats were obtained from Harlan (Indianapolis, IN) and were housed in standard cages with corncob bedding. Rat spinal cord transection was carried out at the age of 7.5 weeks and weight of 270–300 g. Animals had access to food and water ad libitum and were housed individually after surgery. A 12 hour light/dark cycle (lights on at 7:00 am) was used throughout their housing.

2.1. Experimental groups and tissue sample collection

For each time point analyzed (2 weeks and 5 weeks after SCI), four control animals and four animals with complete spinal transection were used as independent samples. Biological replicates in each group of samples or controls (n = 4) were used for microarray analysis, as well as independent biological replicates (n = 4) were prepared for western blot analyses and immunohistochemistry. Lumbar spinal cords and corresponding DRGs were used in all experiments.

2.2. Spinal cord transection

Rats were anesthetized with 1.5–2% isoflurane, placed into a spinal unit apparatus (Stoelting, Wood Dale, IL) and a partial laminectomy of Th8–Th9 vertebra was performed using a dental drill (exposing the dorsal surface of Th10 spinal segment). The spinal cord was then transversally cut using scalpel blade. After transection, the incision was cleaned with 3% H_2O_2 and penicillin/streptomycin mixture and closed in two layers. Animals were then allowed to recover and the presence of spasticity and touch-evoked hyper-reflexia assessed at 7 day intervals (as described in Section 2.2). All animals with spinal transection were treated with antibiotics (cefazolin; 5 mg/kg/day, s.c.) for 10–14 days.

2.3. Identification of muscle spasticity in rats with spinal trauma injury

After spinal transections, animals (n = 4) were tested for the presence of spasticity by measurement of spinal hyper-reflexia after applying two qualitatively different sensory input stimuli:

a) *Touch-evoked muscle hyper-reflexia*: Fully awake animals were placed into a plastic-tube restrainer. Two stainless steel electromyography (EMG) recording electrodes were placed into gastrocnemius muscle 1 cm apart. Using von Frey filaments, a progressively increased force (1–15 g) was then applied into a plantar surface of the left hind limb paw. Before, during, and for 5 s after application of each force test, the EMG signal was recorded and stored on a computer for subsequent analysis. The EMG signal was amplified with an alternating current-coupled differential amplifier (model DB4; World Precision Instruments, Sarasota, FL) and bandpass filtered at 100 Hz to 10 kHz.
b) *Muscle stretch-evoked spasticity*: The presence of muscle spasticity was identified as a velocity-dependent increase in ankle resistance which correlated with increased EMG activity measured in the gastrocnemius muscle during computer-controlled ankle dorsiflexion [9]. Briefly, rats with spinal transection were individually placed in a plastic restrainer, and one hindpaw was securely fastened to the paw attachment metal plate, which was interconnected loosely to the "bridging" force transducer (LCL454G, 0–454 g range; or LCL816G, 0–816 g range; Omega, Stamford, CT). After a 20 min acclimatization period, rotational force was applied to the paw attachment unit using a computer-controlled stepper motor (MDrive 34 with onboard electronics; microstep resolution to 256 microsteps/full step; Intelligent Motion Systems, Marlborough, CT), causing the ankle to dorsiflexion. The resistance of the ankle was measured during 40° of dorsiflexion at progressively increased rotational velocities of 40°, 200° or 400° s^{-1}, and data were collected and analyzed using custom software (Spasticity version 2.01; Ellipse, Kosice, Slovak Republic).

Author's personal copy

2.4. Protein sample collection and preparation

The whole sample preparation procedure was done at 4 °C. The Kinex™ lysis buffer, pH 7.2 containing 20 mM MOPS, 2 mM EGTA, 5 mM EDTA, 30 mM sodium fluoride, 60 mM β-glycerophosphate, 20 mM sodium pyrophosphate, 1 mM sodium orthovanadate, 1 mM phenylmethylsulfonylfluoride, 3 mM benzamidine, 5 μM pepstatin A, 10 μM leupeptin, and 1% Triton X-100 was freshly prepared and kept on ice. Each animal was deeply anesthetized with 100 mg/kg sodium pentobarbital applied intraperitoneally and transcardially perfused with 300 mL of ice cold heparinized (4000 USP units/L) PBS.

Technique of spinal cord tissue and DRG harvest was identical to spinal cord transected and naïve, non-injured animals. To remove lumbar portion of the spinal cord, a 18-gauge needle was attached to a 30-mL syringe that had been filled with ice-cold PBS and the needle tip was inserted into the caudal-most region of the vertebral column, and the buffer was rapidly injected in order to force the spinal cord out through the rostral Th11–12 foramen. DRGs (L2–L6) were rapidly dissected using rongeur. Both isolated lumbar spinal cords and ganglia were snap-frozen in isopentane pre-chilled to −80 °C before further processing.

Whole frozen lumbar spinal cords were then mounted on cryostat holders using mounting media. White matter and the dorsal portion of the gray matter were then trimmed off. Only gray matter ventral horns were harvested, cut to small pieces and directly lyzed in the Kinex™ buffer. DRGs were mounted on cryotome target in the Kinex™ lysis buffer and cut to 30 μm slices. Both tissues were disrupted by sonication in ice cold Kinex™ lysis buffer, and the suspensions were centrifuged at 21,000 *g* for 45 min at 4 °C. The protein concentrations in collected supernatants were determined using BCA assay (Thermo Scientific, Rockford, IL). The protein concentration of each sample was adjusted to 2 mg/mL, DTT was added to final concentration of 1 mM, and the lysates were frozen to −80 °C.

2.5. Antibody microarray

The Kinex™ KAM-1.1 antibody microarray was used to perform an unbiased characterization of signaling proteins that are regulated during sub-acute to chronic phases of SCI. The antibody microarray allowed monitoring of protein levels and/or site-specific protein phosphorylations of kinases, phosphatases and other signaling molecules. In total, this microarray featured 626 antibodies of which 369 were pan-specific and 257 were protein phospho-site-specific. For clarity, all of the numbering of the phospho-sites in this report refer to the human cognates. The Kinex™ KAM-1.1 antibody microarray analyses were performed as described previously [34–36] and according to instructions available on www.kinexus.ca. The antibodies printed on the Kinex™ KAM-1.1 antibody microarray were selected from more than 3000 commercial antibodies that were independently tested by Kinexus for positive western blot signals. The antibodies were also chosen based on their reactivities with target proteins in human, mouse and rat model systems. Briefly, 50 μg of proteins of the control and treated samples were separately labeled with the same fluorescent dye and unincorporated dye molecules were removed by ultrafiltration. Purified labeled proteins from two samples were incubated separately on the opposite ends of antibody microarray as the microarray featured two identical fields of antibody grids and 652 antibody duplicates were printed within each field. After washing, arrays were scanned using a Scan Array Express Reader (Perkin Elmer, Wellesley, MA) with a resolution of 10 μm, and acquired images were quantified using ImaGene software (BioDiscovery, El Segundo, CA).

2.6. Microarray data analysis

The net signal median for each antibody spot was obtained by subtraction of the background from signal intensity of the spot. For the spots with median signal values lower than background, net signal median value equal to 1 was assigned to avoid negative values in follow-up analysis. The quality of all microarrays was then verified computationally. The values of net signal medians were normalized by multiplying with the normalization coefficient, calculated for each of the two samples measured on one array as average sum of net signal medians of all spots on array divided by sum of net signal medians corresponding to individual sample on the array. The calculated values of normalized net signal medians for individual spots were part of the report provided by Kinexus service. Such normalization allowed comparison of groups and further statistical analysis. The normalized net signal medians of two on-array duplicates for each antibody were then averaged. The variances in averaged normalized net signal medians between control and transected spinal cord samples were compared using F-test for each time-point and tissue type. According to F-test results, unpaired two-sample *t*-test for populations with equal or unequal variance was calculated and differences between control and experimental samples (n = 4 for each group) with $p < 0.05$ were considered as significant. Signal-to-noise ratios (SNRs) of individual antibody spots on the array were calculated by dividing the signal and background intensities. The SNRs of each sample type (4 biological replicates with 2 on-array duplicates) were averaged and the proteins with SNRs in both control and treated samples below stringent cut-off value of 1.5 were removed from the list of different proteins in order to consider unambiguous spots with higher signal intensity on the microarray.

2.7. Bioinformatic evaluation of quantitative microarray

To characterize and visualize the impact of spinal transection at the time point of resultant spasticity into cellular signaling networks, UniProtKB accession numbers of regulated (phospho) proteins were submitted to the PANTHER database (Version 7.2, release date 2012-03-16, www.pantherdb.org) [37]. The PANTHER Pathway, consisting of over 175 primarily signaling pathways, was used to determine the distribution of significantly regulated proteins among individual signaling pathways. In case the protein was not assigned to any signaling pathway, its classification according to the PANTHER biological process was used. To investigate distributions in affected signaling pathways, chi-squared test was calculated with respect to the number of on-array proteins and differences between the

Author's personal copy

expected and observed frequencies with $p < 0.05$ were considered as significant.

Interologous Interaction Database (I2D) of known and predicted mammalian and eukaryotic protein–protein interactions (Version 1.95, release date 2012-02-02, http://ophid.utoronto.ca) [38] was queried online via a web interface to search for possible interaction partners with human selected as a target organism with respect to the numbering in Kinexus array, which refers to the human cognates. Protein–protein interaction networks were visualized using NAVIGaTOR 2.2.1 (http://ophid.utoronto.ca/navigator/). In protein–protein interaction networks, nodes represent proteins and edges between nodes represent physical interactions between proteins.

2.8. Western blotting

Tissue lysates for western blotting were prepared using SDS lysis buffer containing 31.25 mM Tris–HCl (pH 6.8), 1% SDS (w/v), 12.5% glycerol (v/v), 0.02% bromophenol blue (w/v), and 1.25% β-mercaptoethanol, boiled for 4 min at 100 °C, and then frozen to −80 °C. The western blots were performed using Kinetworks™ KCSS-1.0 Screen service (www.kinexus.ca). The primary antibodies to detect macrophage-stimulating protein receptor alpha chain (RONα), HSP27 and PKCδ were selected and diluted 1:500 or to a final concentration of 2 μg/ml for this analysis. Chemiluminescence signals were captured by a Fluor-S Multiimager and quantified using Quantity One 4.6.5 (Bio-Rad, Hercules, CA). The Trace Quantity of a band was determined by the area under its intensity profile curve (intensity × mm). The C.P.M. (count per minute) value was calculated as the trace quantity of the band corrected to what a scan time would yield if it was of 60 s duration. Unpaired two-sample *t*-test for populations with equal variance was calculated to compare C.P.M. values of control and spinal trauma samples and *p*-values are shown in Fig. 4.

2.9. Immunohistochemistry

The animals were deeply anesthetized with pentobarbital (100 mg/kg) and perfused by 250 mL of ice-cold heparinized PBS containing phosphatase inhibitors (PBS + Inh) including 1 mM β-glycerophosphate, 5 mM sodium fluoride, 1 mM sodium orthovanadate, 10 mM sodium pyrophosphate, followed by 250 mL of 4% (v/v) paraformaldehyde in PBS + Inh. The spinal cords with adjacent tissue were dissected and post-fixed in 4% paraformaldehyde in PBS + Inh at 4 °C for additional 48 h. The DRGs and the lumbar spinal cords were isolated and incubated for 48 h in 15 mL of 30% (w/v) sucrose in PBS at 4 °C. The cryoprotected tissue was frozen in isopentan and 30 μm sections cut on Leica cryotome. The lumbar spinal cord sections were stained as floating sections, the ganglia sections were mounted and stained on glass slides. The sections were washed in PBS + Inh, blocked for 1 h in 5% (v/v) donkey serum in PBS + Inh, washed in PBS + Inh and incubated overnight at 4 °C in primary antibody dissolved in PBS containing 0.3% (v/v) Triton X-100. After washing in PBS, sections were incubated for 1 h with secondary antibody diluted 1:250 in PBS. Primary antibodies recognizing pan-specific RONα, HSP27 and PKCδ as well as known neural cell markers GFAP, Iba1, ChAT, NeuN and APC-Alexa 647 conjugates were used (Supplementary Table 1). As secondary antibodies, DyLight 488-, 549- or 649-conjugated AffiniPure F(ab′)$_2$ Fragment of Donkey Anti-Rabbit, Anti-Mouse or Anti-Goat IgG (H + L) (Jackson Immunoresearch, Suffolk, UK) were used. Nuclei were stained by DAPI (0.1% w/v) in PBS-TX for 10 min. After final washing in PBS containing 0.3% (v/v) Triton X-100, the spinal cord sections were mounted on glass slides, all sections were overlaid by ProLong® Gold Antifade Reagent (Life technologies, Carlsbad, CA) and covered by cover slips. Images were captured by Olympus Fluoview FV1000 confocal microscope and visualized in FV10-ASW, Version 2, software (Olympus, Tokyo, Japan).

3. Results

3.1. Spinal Th9 transection leads to progressive appearance of touch-evoked hyper-reflexia and velocity of muscle stretch-dependent spasticity

3.1.1. Touch-evoked hyper-reflexia

Rats with previous Th9 transection showed a time-dependent appearance of touch-evoked muscle hyper-reflexia as evidenced by measured burst EMG activity in the gastrocnemius muscle immediately after applying the mechanical stimulus on the plantar surface of the paw. Progressive increase in paw compression force from 3 to 15 g evoked a clear increase in EMG activity measured in gastrocnemius muscle. Positive EMG responses were consistently measured at compression pressures ≥2 g at 3–5 weeks after SCI (Fig. 1A, B, C). In contrast, in control animals no response was measured at pressures up to 15 g (data not shown). A comparable exacerbated EMG responses were measured in the left and right gastrocnemius muscle.

3.1.2. Muscle stretch-dependent spasticity

Similar to touch-evoked hyper-reflexia, the appearance of muscle spasticity was measured at intervals 3–5 weeks after spinal transection. The presence of spasticity was identified by burst EMG activity and concomitant increase in ankle resistance measured during computer-controlled ankle dorsiflexion from 0 to 40° (Fig. 1D). Increase in ankle rotational velocity from 40° s^{-1} to 400° s^{-1} led to a clear increase in EMG response and correlative increase in ankle resistance (Fig. 1E–F transected; EMG and ankle resistance). In addition, long-lasting EMG activity lasting for 1–3 s after ankle rotation was seen in 3 of the 4 animals.

3.2. Utilization of the antibody microarray approach for the analysis of spinal cellular signaling proteins

Protein extracts were prepared from lumbar spinal ventral horns 2 weeks after SCI, lumbar spinal ventral horns 5 weeks after SCI, lumbar DRGs 5 weeks after SCI and control SHAM-operated ventral horns and DRGs. Each group consisted of 8 samples including 4 samples prepared from 4 animals with complete Th9 transection and 4 samples prepared from control SHAM-operated animals. The consistency of antibody microarray assay was demonstrated by plotting the normalized net signal median values for two replicates of each

Author's personal copy

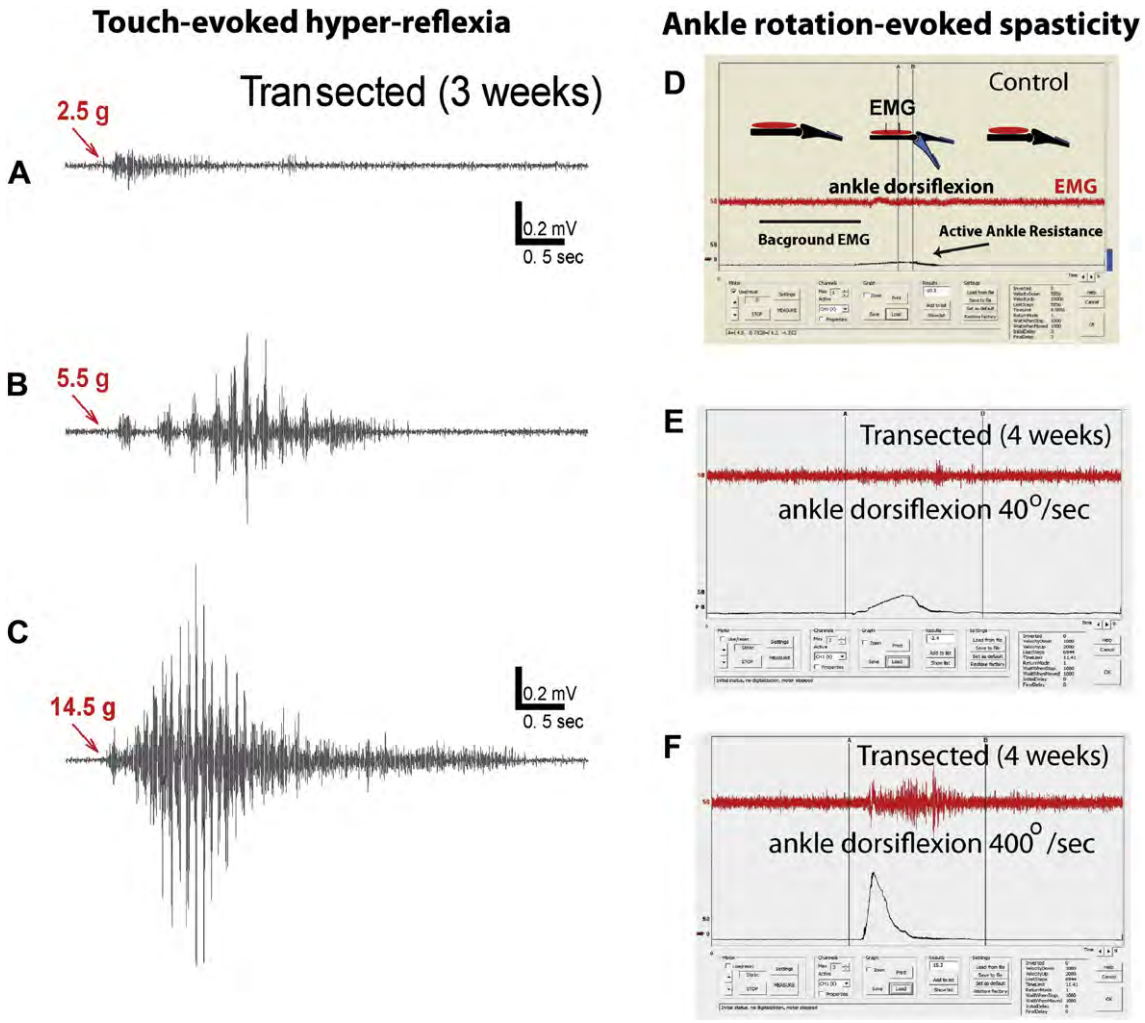

Fig. 1 – Development of touch-evoked hyper-reflexia and ankle-rotation-evoked muscle spasticity in rats after Th9 spinal transection. (A–F) In fully awake restrained animals mechanical force was applied into plantar surface of the paw using von Frey filaments. Compression force-dependent increase in EMG response was seen at intervals from 3 weeks after spinal transection (A–C). To identify the presence of muscle spasticity ankle rotational force was applied in fully awake animals and ankle rotated 40° at progressively increased ankle rotational velocities (40° → 200° → 400°/s) and EMG activity and corresponding ankle resistance measured using digital transducer (D). At high rotational velocities, a clear exacerbated EMG response and resulting increase in muscle resistance was measured at 40°/s rotation (E) and at 400°/s rotation (F).

antibody that revealed correlation with the values of coefficients of determination (R^2) from 0.89 to 0.64 and median 0.81 (Supplementary Fig. 1). The highest intensity signal observed was 25,500 counts, and the lowest reproducible signal was 225 counts thus providing 100-fold range of linear detection of protein binding in Kinex™ antibody microarray. The net signal medians of all spots captured on individual chip were normalized using normalization coefficients which ranged from 0.77 to 1.23 with median value 1.00 for all chips. Consequently, 1.2 and higher fold changes in averages of normalized net signal medians between two compared samples were deemed to be a potential alteration in either protein turnover or phosphorylation between these samples. The significance of low fold change values was corroborated by *p*-value of 0.01 while for the spots with fold change 1.5 higher *p*-value of 0.05 was applied. For simplification of the result outcome, it is assumed that the pan-specific antibodies tracked changes in protein levels, and the phospho-site antibodies monitored the phosphorylation status of specific phospho-sites in target proteins [39]. The performance of several hundreds of antibodies used by Kinexus on their Kinex ™ antibody microarray is available in open-access KiNET-IB website (www.kinet.ca).

3.3. *Overview of protein level/phosphorylation changes in lumbar spinal ventral horns and dorsal root ganglion cells caudal to spinal transection*

The lists of averaged normalized net signal medians for all antibody spots in all analyzed samples together with

Author's personal copy

Table 1 – Changes in regulation of protein species up to 5 weeks after spinal transection.

Serial no.	UniProtKB accession	Protein name	Phospho-site	Fold change	SCI
1139	P23443	p70/p85 ribosomal protein-serine S6 kinase alpha	T229	1.45	2 weeks
1141	P23443	p70/p85 ribosomal protein-serine S6 kinase alpha	T421 + S424	−1.24	5 weeks
1119	Q15418	Ribosomal S6 protein-serine kinase 1/2	S221/S227	1.25	5 weeks
1121	Q15418	Ribosomal S6 protein-serine kinase 1/2	S363/S369	−1.30	5 weeks
555	P45983	Jun N-terminus protein-serine kinase	T183/Y185	−1.21	5 weeks
553	P45983	Jun N-terminus protein-serine kinases	Pan-Specific	−1.85	5 weeks
441	P04792	Heat shock 27 kDa protein beta 1 (HspB1)	Pan-Specific	1.39	5 weeks
447	P04792	Heat shock 27 kDa protein beta 1 (HspB1)	S15	−1.39	5 weeks
445	P04792	Heat shock 27 kDa protein beta 1 (HspB1)	S15	−1.37	5 weeks
591	P06239	Lymphocyte-specific protein-tyrosine kinase (Lck)	Pan-Specific	−1.58	5 weeks
595	P06239	Lymphocyte-specific protein-tyrosine kinase (Lck)	S157	−1.86	5 weeks

summary statistics are shown in Supplementary Table 2. A statistical microarray data analysis revealed 85 significant protein level/phospho-site protein phosphorylation changes with minimal fold change ±1.2 and $p < 0.05$ present in at least one of three treated sample groups compared to corresponding controls in rat spinal cord transection model of spasticity evolved up to 5 weeks after injury (Supplementary Table 3).

These changes represented 13.6% of all 626 antibodies used in this study. Among these significant changes, 2 proteins (2.36%) and 1 protein phosphorylation (1.18%) were increased while 4 proteins (4.71%) and 2 protein phosphorylations (2.36%) were decreased in lumbar spinal ventral horns 2 weeks after SCI (Supplementary Table 3A). More noticeable were the changes typical for lumbar spinal ventral horns 5 weeks after SCI including increased levels of 16 proteins (18.82%) and 12 phospho-site protein phosphorylations (14.12%), while 30 proteins (35.29%) and 14 protein phosphorylations (16.47%) were decreased (Supplementary Table 3B). Typical for DRGs 5 weeks after SCI, decreases were noticed in the levels of 3 proteins (3.53%) and 1 protein phosphorylation (1.18%) (Supplementary Table 3C).

Despite distinct numbers of protein changes in observed time intervals and locality, there was only one protein that decreased in 5 weeks after SCI, namely, STE20-like protein-serine kinase (UniProtKB access. Q9UHG7) which overlapped between lumbar spinal ventral horns and DRGs (Supplementary Table 3D). This confirmed considerable distinct spatial distribution of protein changes in spinal cord caudal to the region of transection. As regards temporal changes, no regulated protein levels or protein phosphorylations common to lumbar spinal ventral horns were observed 2 and 5 weeks after SCI, possibly indicating dynamic course of evolving spasticity after spinal transection. Interestingly, five proteins exhibited the changes of their different species, which were mainly apparent in ventral horns 5 weeks after SCI, except for different phospho-sites of p70/p85 ribosomal protein-serine S6 kinase alpha observed also at 2 weeks after SCI (Table 1).

From the experimental results obtained, it was evident that decreases mainly in protein levels (44% of all changes) and down-regulation of phospho-site protein phosphorylations (20% of all changes) were dominant compared to increases in protein levels. Apparently, the highest number of changes observed in lumbar spinal ventral horns 5 weeks after SCI (Supplementary Table 3B), timely correlated with appearance of functional/mechanical signs of spasticity as identified by increase in ankle resistance during computer-controlled ankle dorsiflexion and increase in EMG activity in the gastrocnemius muscle (Fig. 1). With a variety of significant changes in protein levels and phospho-site protein phosphorylations, we further focused on: (i) marked changes observed relative to maximum fold change and significance; (ii) regulatory proteins/protein phosphorylations involvement in cellular signaling pathways; and (iii) protein–protein interaction network connections to the regulated proteins after spinal transection.

3.4. *The most marked protein changes observed in spinal ventral horns and dorsal root ganglion cells related to spasticity appearance during secondary damage after spinal injury*

From our experimental results, it was evident that the number of marked protein changes observed up to 5 weeks after spinal injury was not high (Table 2). Such changes included up-regulation of CaMKIV and down-regulation of MAPK/ERK kinase kinase 4 (MEKK4), MAPK/ERK kinase kinase 2 as well as focal adhesion protein-tyrosine kinase (FAK) phosphorylation on Ser843 which were observed 2 weeks after trauma.

The most marked difference appeared to be the increased phosphorylation on Ser1107 of eukaryotic translation initiation factor 4 gamma (eIF4G) 5 weeks after trauma reflecting only one protein change fulfilling most stringent criteria of fold change >2 and $p < 0.01$ (Table 2A). The increase in the level of striatin-3 and decrease of insulin-like growth factor receptor (IGFR) were among the most marked changes observed in lumbar spinal ventral horns at 5 weeks after SCI (Table 2B).

In total, 28 significant changes were observed in ventral horns with fold change >1.2 and $p < 0.01$ (Table 2C). Two proteins including preimplantation protein 3 and RONα, and four phospho-site changes such as microtubule-associated protein tau (Ser515) and ribosomal S6 protein-serine kinase 1/2 (Ser221/Ser227) were increased. Among 15 decreasing levels of proteins, lymphocyte-specific protein-tyrosine kinase (Lck) and angiopoietin-1 receptor-tyrosine kinase (TEK/TIE2) represented the most significant changes. Additionally, the known proteins of several signaling cascades such as JNK1/2/3 or PKCδ were identified. Interestingly, three apoptotic proteases, pro-caspase 6, 7 and 9 (CASP6, CASP7 and CASP9) were

Author's personal copy

Table 2 – The most marked protein level/phosphorylation changes in ventral horns of spinal parenchyma up to 5 weeks after spinal transection.

Serial no.	UniProtKB accession	Target protein	Full target protein name	Phospho site	Fold change	*p*-Value	SCI
A. Fold change > 2.00 and p < 0.01							
299	Q04637	eIF4G	Eukaryotic translation initiation actor 4 gamma 1	S1107	2.01	0.0031	5 weeks
B. Fold change > 2.00 and p < 0.05							
113	Q16566	CaMKIV	Calcium/calmodulin-dependent protein-serine kinase 4	Pan-specific	2.30	0.0117	2 weeks
681	Q9Y6R4	MEKK4	MAPK/ERK kinase kinase 4	Pan-specific	−2.02	0.0187	2 weeks
351	Q05397	FAK	Focal adhesion protein-tyrosine kinase	S843	−2.01	0.0489	2 weeks
1147	Q13033	SG2NA	Striatin-3	Pan-specific	2.60	0.0141	5 weeks
491	P08069	IGF1R	Insulin-like growth factor receptor protein-tyrosine kinase	Pan-specific	−2.45	0.0259	5 weeks
C. Fold change > 1.20 and p < 0.01							
679	Q9Y2U5	MEKK2	MAPK/ERK kinase kinase 2	Pan-specific	−1.63	0.0077	2 weeks
1109	Q04912	RONα	Macrophage-stimulating protein receptor alpha chain	Pan-specific	1.90	0.0017	5 weeks
699	Q9Y3A3	mMOB1	Preimplantation protein 3	Pan-specific	1.70	0.0003	5 weeks
1297	P43403	ZAP70	Zeta-chain (TCR) associated protein-tyrosine kinase, 70 kDa	Y315 + Y319	1.39	0.0027	5 weeks
645	Q02750	MEK1	MAPK/ERK protein-serine kinase 1 (MKK1)	T385	1.37	0.0041	5 weeks
1225	P10636	Tau	Microtubule-associated protein tau	S515	1.30	0.0048	5 weeks
1119	Q15418	RSK1/2	Ribosomal S6 protein-serine kinase 1/2	S221/S227	1.25	0.0085	5 weeks
553	P45983	JNK1/2/3	Jun N-terminus protein-serine kinases (stress-activated protein kinase (SAPK)) 1/2/3	Pan-specific	−1.85	0.0062	5 weeks
511	Q13418	ILK1	Integrin-linked protein-serine kinase 1	Pan-specific	−1.73	0.0075	5 weeks
331	P30101	ERP57	ER protein 57 kDa (protein disulfide isomerase-associated 3; 58 kDa glucose regulated protein)	Pan-specific	−1.65	0.0011	5 weeks
551	Q9UHG7	JIK	STE20-like protein-serine kinase	Pan-specific	−1.59	0.0094	5 weeks
591	P06239	Lck	Lymphocyte-specific protein-tyrosine kinase	Pan-specific	−1.58	0.0002	5 weeks
1247	Q02763	TEK/TIE2	Angiopoietin-1 receptor-tyrosine kinase	Pan-specific	−1.56	0.0005	5 weeks
213	P68400	CK2a	Casein protein-serine kinase 2 alpha/alpha prime	Pan-specific	−1.55	0.0033	5 weeks
1287	P30291	Wee1	Wee1 protein-tyrosine kinase	Pan-specific	−1.52	0.0049	5 weeks
915	Q05655	PKCδ	Protein-serine kinase C delta	Pan-specific	−1.49	0.0097	5 weeks
133	P55212	CASP6	Pro-caspase 6 (apoptotic protease Mch2)	Pan-specific	−1.43	0.0075	5 weeks
563	P05412	Jun	Jun proto-oncogene-encoded AP1 transcription factor	Pan-specific	−1.41	0.0054	5 weeks
253	P53355	DAPK1	Death-associated protein kinase 1	Pan-specific	−1.39	0.0055	5 weeks
135	P55210	CASP7	Pro-caspase 7 (ICE-like apoptotic protease 3 (ICE-LAP3), Mch3)	Pan-specific	−1.34	0.0075	5 weeks
139	P55211	CASP9	Pro-caspase 9 (ICE-like apoptotic protease 6 (ICE-LAP6), Mch6, APAF3)	Pan-specific	−1.32	0.0077	5 weeks
595	P06239	Lck	Lymphocyte-specific protein-tyrosine kinase	S157	−1.86	0.0042	5 weeks
41	Q13315	ATM	Ataxia telangiectasia mutated	S1981	−1.76	0.0008	5 weeks
1153	Q06124	SHP2	Protein-tyrosine phosphatase 1D (SHPTP2, Syp, PTP2C)	S576	−1.50	0.0090	5 weeks
7	P00519	Abl	Abelson proto-oncogene-encoded protein-tyrosine kinase	Y412	−1.37	0.0100	5 weeks
219	Q9Y281	Cofilin 2	Cofilin 2	S3	−1.37	0.0041	5 weeks
1121	Q15418	RSK1/2	Ribosomal S6 protein-serine kinase 1/2	S363/S369	−1.30	0.0057	5 weeks
177	P06493	CDK1/2	Cyclin-dependent protein-serine kinase 1/2	T161/T160	−1.23	0.0050	5 weeks

decreased. As regards phospho-site changes, seven were decreased including Lck on Ser157 (Table 2C).

None of the proteins/protein phosphorylation changes met the above mentioned criteria of most marked changes in DRGs 5 weeks after SCI.

3.5. *Bioinformatic evaluation of antibody microarray data to assign relevant signaling pathways*

With a variety of significant changes in protein levels and protein phosphorylations detected using the Kinex™ KAM-1.0

Author's personal copy

antibody microarray, the importance of such alterations in spinal cellular signaling in the rat with spinal injury-induced spasticity was investigated using the PANTHER database. The major pathways with ten or larger numbers of regulated proteins are listed in Table 3. Among significantly regulated ($p < 0.05$) are those related to angiogenesis, neurodegeneration, integrin signaling, RAS pathway, growth factor signaling (fibroblast growth factor, platelet derived growth factor), and FAS pathway. Subsequent pathways of importance with 5 to 9 regulated proteins included the interferon-gamma signaling, insulin/IGF, endothelin, interleukin and p53 pathways, vascular endothelial growth factor signaling, inflammation mediated by chemokines and cytokines, B cell and T cell activation, oxidative stress response, Toll-like receptor signaling, p38 MAPK and transforming growth factor beta signaling.

The pronounced pathway with the highest number of observed protein alterations was angiogenesis (Tables 3 and 4). The regulated proteins (Fig. 2) included decrease in important up-stream components of this signaling pathway such as TEK/TIE2 and fibroblast growth factor receptor (FGFR) as well as IGFR [40]. Furthermore, many intermediate signaling components including the level of PKCδ and MAPKs (JNK1/2/3, MAPK3/Erk1 Thr202 + Tyr204, p38) were involved. Most importantly, several of the down-stream proteins of the angiogenesis pathway, and therefore likely to have more selective biological effects, included decreased levels of transcription factor Jun and CASP9 as well as lower phosphorylation of endothelial nitric oxide synthase (eNOS) on Thr495, while the level of small HSP protein HSP27 was increased although its phosphorylation on Ser15 was decreased (Table 1).

Another significant pathway of the top regulated spinal cellular signaling in rat with spinal injury-induced spasticity was the neurodegeneration pathway (Tables 3 and 5). In case of the Jun, JNK1/2/3, Src, PKCδ, p38 MAPK, MEK4, PKBα and Erk1 proteins that were assigned to angiogenesis but also related to neurodegenerative disease pathways (Tables 4 and 5), where it was evident that these proteins participated in the cross-talk of a variety of cellular signaling pathways (Supplementary Table 3). More importantly, distinct proteins that appeared to be more selectively related to the neurodegenerative diseases were recognized (Table 5). According to PANTHER, the participation of the Lck and Lyn kinases, as well as casein protein-serine kinases (CK2a and CK1g2) was evident and these proteins were mainly assigned to Parkinson disease. Furthermore, the CASP6 and CASP8, which appeared to be selective for the Huntington disease pathway, were down-regulated.

3.6. Model of protein–protein interaction network connecting angiogenesis and neurodegeneration signaling after spinal transection

The selective proteins differentially regulated during secondary damage and evolving spasticity up to 5 weeks after spinal transection were introduced into I2D database in order to graphically visualize possible functional relationships among these molecules (Fig. 3). Only the proteins that were assigned by PANTHER either to angiogenesis pathway (Table 4; FAK, TEK/TIE2, CASP9, SHP2, eNOS, FGFR, HSP27, Crystallin αB) or neurodegeneration (Table 5; Lck, CK2a, CK1g2, CASP6, Lyn, CASP8) but not to both processes, were implemented in this evaluation.

In total, 1427 interactions were recognized for 14 selected proteins mentioned above. Computer modeling highlighted direct interactions between angiogenesis regulating proteins FAK and TEK/TIE2, and the Lck and Lyn kinases involved in neurodegenerative pathway, which may form the central hub of the network. Furthermore, interactions of protein phosphatase SHP2 with Lck as well as CASP9 with CASP8 were identified in the connecting of angiogenic and neurodegenerative pathways. Direct interconnections between these proteins were further extended by high number of indirect interactions. Contrary to this, the FGFR, eNOS, Crystallin αB and HSP27 involved in regulation of angiogenesis and CK2a, CK1g2 and CASP6 regulating neurodegeneration, remained segregated from the key central interaction network.

3.7. Verification of differentially expressed proteins RONα, HSP27 and PKCδ using western blot analysis

Using Kinex™ microarrays, non-denatured proteins were analyzed, and this increased the possibility of false positives and false negatives due to antibody cross-reactivity and blocked epitopes in protein complexes, respectively. Therefore, several candidate changes observed on Kinex™ microarrays were selected for verification by western blotting. Importantly, we focused mainly on the altered proteins that may potentially serve as new targets in developing treatment strategies.

Immunoblot experiments were performed to verify relevant protein changes: RONα (Table 2), HSP27 (Table 4; Figs 2 and 3) and PKCδ (Tables 2, 4 and 5; Fig. 2). The results shown in Fig. 4 confirmed significantly higher levels of RONα and HSP27 in ventral horns 5 weeks after transection. Contrary to the

Table 3 – Signaling pathways with the highest number of protein alterations after spinal transection.

Signaling pathway (PANTHER 7.2)	No. of regulated proteins	No. of on-array proteins	p-Value
Angiogenesis (P00005)	17	54	0.0010
Neurodegeneration (P00049, P00003, P00029)	16	65	0.0216
Integrin signaling pathway (P00034)	14	30	2.75×10^{-05}
Apoptosis signaling pathway (P00006)	13	61	0.1159
Fibroblast growth factor signaling pathway (P00021)	12	33	0.0017
Ras pathway (P04393)	12	42	0.01556
Platelet derived growth factor signaling pathway (P00047)	11	42	0.0401
Epidermal growth factor signaling pathway (P00018)	11	49	0.1115
FAS signaling pathway (P00020)	10	17	4.21×10^{-05}

Author's personal copy

Table 4 – Regulated proteins/phosphoproteins in angiogenesis pathway (P00005) assigned by PANTHER 7.2.

Serial no.	UniProtKB accession	Target protein	Full target protein name	Phospho-site	Fold change	*p*-Value	SCI
1247	Q02763	TEK/TIE2	Angiopoietin-1 receptor-tyrosine kinase	Pan-specific	−1.56	0.0005	5 weeks
563	P05412	Jun	Jun proto-oncogene-encoded AP1 transcription factor	Pan-specific	−1.41	0.0054	5 weeks
553	P45983	JNK1/2/3	Jun N-terminus protein-serine kinases (stress-activated protein kinase (SAPK)) 1/2/3	Pan-specific	−1.85	0.0062	5 weeks
139	P55211	CASP9	Pro-caspase 9 (ICE-like apoptotic protease 6 (ICE-LAP6), Mch6, APAF3)	Pan-specific	−1.32	0.0077	5 weeks
1153	Q06124	SHP2	Protein-tyrosine phosphatase 1D (SHPTP2, Syp, PTP2C)	S576	−1.50	0.0090	5 weeks
915	Q05655	PKCδ	Protein-serine kinase C delta	Pan-specific	−1.49	0.0097	5 weeks
667	P45985	MEK4	MAPK/ERK protein-serine kinase 4 (MKK4)	S257 + T261	−1.55	0.0114	2 weeks
555	P45983	JNK	Jun N-terminus protein-serine kinase (stress-activated protein kinase (SAPK))	T183/Y185	−1.21	0.0242	5 weeks
301	P29474	eNos	Nitric-oxide synthase, endothelial	T495	−1.55	0.0368	5 weeks
361	P11362	FGFR1	Fibroblast growth factor receptor-tyrosine kinase 1	Pan-specific	−1.28	0.0372	5 weeks
441	P04792	HSP27	Heat shock 27 kDa protein beta 1 (HspB1)	Pan specific	1.39	0.0388	5 weeks
1181	P12931	Src	Src proto-oncogene-encoded protein-tyrosine kinase	Y529	1.26	0.0451	5 weeks
779	Q16539	p38a MAPK	Mitogen-activated protein-serine kinase p38 alpha	Pan-specific	1.37	0.0478	5 weeks
881	P31749	Akt1	Protein-serine kinase B alpha	T308	1.43	0.0485	5 weeks
351	Q05397	FAK	Focal adhesion protein-tyrosine kinase	S843	−2.01	0.0489	2 weeks
317	P27361	Erk1	Extracellular regulated protein-serine kinase 1 (p44 MAP kinase)	T202 + Y204; T185/Y187	1.32	0.0489	5 weeks
235	P02511	Crystallin aB	Crystallin alpha B (heat-shock 20 kDa like-protein)	S45	−1.53	0.0490	5 weeks

decrease in PKCδ level observed on microarray, western blot showed significant increase of this protein. This may reflect increased interactions of PKCδ within complexes.

3.8. *Localization of differentially expressed proteins RONα, HSP27 and PKCδ*

Selected proteins were further investigated for their cellular localization within specific neural cell types using immunohistochemistry. Co-staining was performed with currently accepted markers such as NeuN typical for neuronal nuclei, ChAT indicating cholinergic neurons, particularly α-motoneurons in ventral horns, Iba1 typical for microglia, GFAP for staining astrocytes and APC showing oligodendrocytes that may be present in spinal ventral horn sections. According to immunohistochemical observations, the expansion of GFAP-positive astrocytes and Iba1-positive microglia were characteristic for response to SCI up to 5 weeks after trauma.

The expression of RONα in spinal cord evidently increased after SCI. While in control spinal cord the RONα remained undetectable in both gray and white matter, two weeks after SCI several RONα positive cells appeared in the gray matter (Fig. 5A′; arrowheads). In addition, the RONα expression at 5 weeks after SCI was markedly induced in the white matter (Fig. 5A″), where the protein was localized in GFAP positive astrocytes (Fig. 5B″). As the RONα receptor is typically expressed on macrophages [41], we examined the RONα expression in microglia, which represents endogenous macrophage lineage present in the central nervous system. However, there was no co-localization of RONα with microglial marker Iba1 (Fig. 5C–C″).

In both control and trauma spinal cords, HSP27 was expressed in cytoplasm of large ChAT and NeuN positive cells (α-motoneurons) in ventral horns (Supplementary Fig. 2A, A′, B, B′). The spinal cord trauma induced HSP27 expression in additional large NeuN positive but ChAT negative neurons distributed over the gray matter (Supplementary Fig. 2A′ and 2B′; arrowheads). In the white matter, HSP27 levels in astrocytes notably increased 5 weeks after SCI (Supplementary Fig. 2C, C′).

In spinal ventral horns of control and SCI samples, PKCδ was expressed in large ChAT positive motoneurons (Supplementary Fig. 3A–A″). After SCI, the PKCδ expression was induced in small cells of irregular shape distributed in both gray (Supplementary Fig. 3B–B″) and white matter (Supplementary Fig. 3C–C″ and 3D–D″). These cells were negative for NeuN and GFAP staining of neurons and astrocytes, respectively. In the white matter adjacent to ventral horns, several PKCδ positive cells were positive for APC marker of mature oligodendrocytes (Supplementary Fig. 3D–D″, arrowheads). The remaining PKCδ positive, but NeuN, GFAP or APC-negative cells might represent microglia.

4. Discussion

Development of progressive muscle spasticity also known as exacerbated muscle contraction after increasing velocity of

Author's personal copy

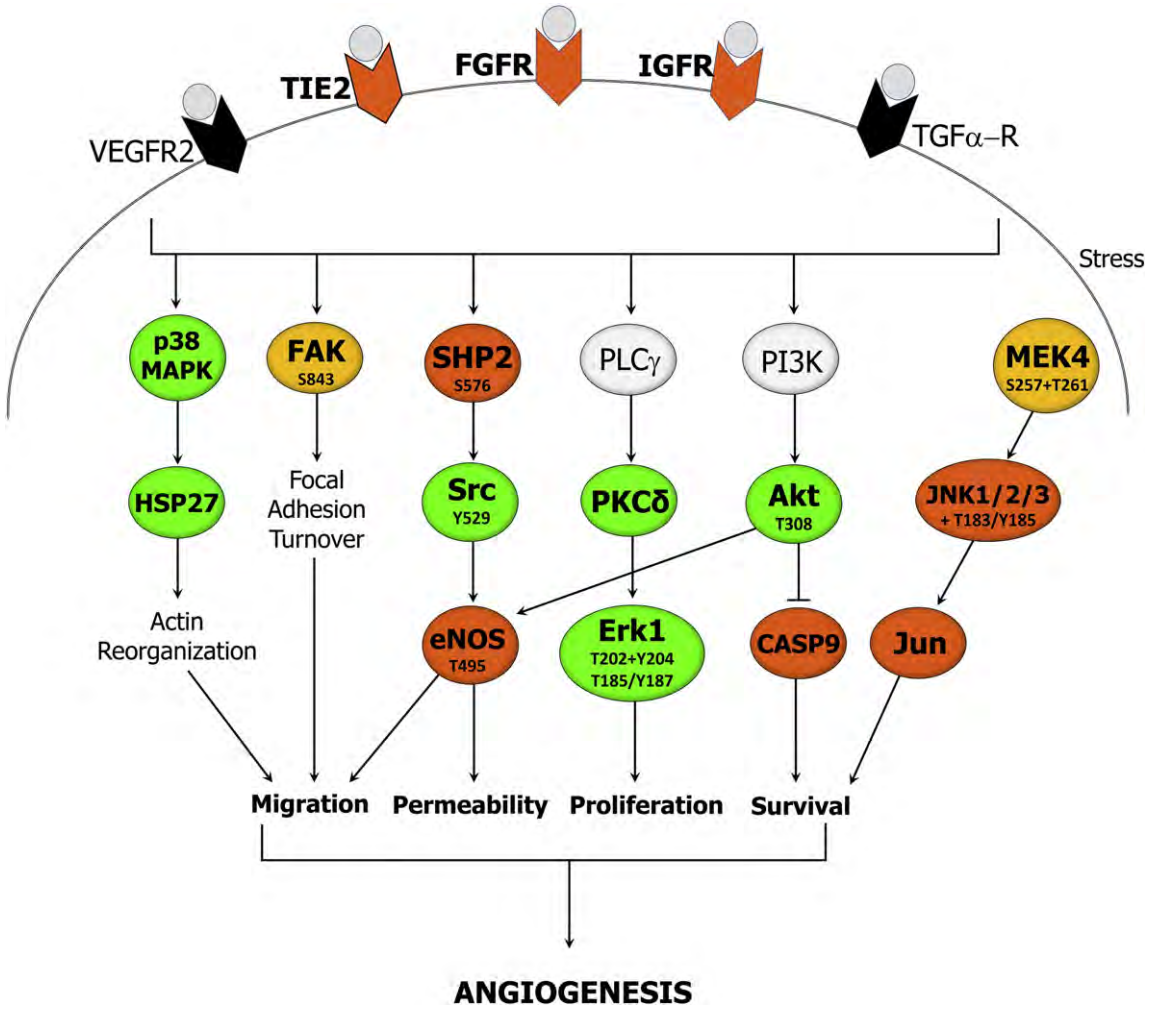

Fig. 2 – Angiogenesis signaling pathway regulation in the rats after Th9 spinal transection with resultant spasticity. To visualize the impact of spinal transection on angiogenesis, majority of proteins assigned to this pathway by PANTHER database were depicted in the model schematic. The protein phosphorylation decreases typical for 2 weeks after transection are in yellow circle, while decreased and increased protein levels/phosphorylations typical for 5 weeks after transection are indicated by red and green colors, respectively. Black and white shapes represent the components of the signaling pathway, which were not measured or changed. The attenuated capacity to trigger angiogenesis via up-stream receptors appears to be counterbalanced by promoting pro-angiogenic effects of effector molecules such as HSP27 and phosphorylated Erk1 as well as decreases in CASP9 level and inhibitory phosphorylation of eNOS.

muscle stretch, represents a serious complication associated with spinal traumatic injury [42]. Importantly, even in partial spinal cord injuries in which a substantial motor function capacity is preserved, the presence of spasticity can significantly alter its effective functional utilization despite ongoing and aggressive physical rehabilitation [43]. In addition to spinal trauma, several other neuropathological conditions which lead to a partial or complete functional loss of the inhibitory neuronal circuits which control spinal segmental α-motoneuron excitability, can lead to the development of clinically-defined spasticity including amyotrophic lateral sclerosis, multiple sclerosis, cerebral palsy, or brain traumatic injury [44–47].

In addition to a defined role of altered segmental inhibition in the evolution of the spasticity state, it is well established that the appearance of a hyperaesthesia such as tactile or thermal hypersensitivity is equally important in the clinical presentation of the spasticity state. Accordingly, clinical studies have shown that the use of dorsal rhyzotomy (surgical transection of segmental dorsal roots to eliminate sensory input) is highly effective in ameliorating the spasticity resulting from spinal trauma, cerebral palsy or multiple sclerosis [48,49]. Thus the definition of pathophysiological/pathobiochemical changes affecting both neurons and glia and residing in spinal cord and DRGs are important as they can serve to delineate a relative contribution of these functionally and anatomically distinct cell populations in the development of chronic spasticity.

In the present study we have analyzed the changes in protein expression in spinal cord parenchyma and corresponding segmental DRGs at 2 and 5 weeks after spinal transections, the time points which coincide with the appearance of clinically defined spasticity. Our findings showing eIF4G Ser1107 hyperphosphorylation and typical decreases in protein levels

Author's personal copy

Table 5 – Regulated proteins/phosphoproteins involved in neurodegeneration pathways (Parkinson disease (P00049), Alzheimer disease-amyloid secretase pathway (P00003), Huntington disease (P00029)) assigned by PANTHER 7.2.

Serial no.	UniProtKB accession	Target protein	Full target protein name	Phospho site	Fold change	*p*-Value	SCI
591	P06239	Lck	Lymphocyte-specific protein-tyrosine kinase	Pan-specific	−1.58	0.0002	5 weeks
213	P68400	CK2a	Casein protein-serine kinase 2 alpha/alpha prime	Pan-specific	−1.55	0.0033	5 weeks
595	P06239	Lck	Lymphocyte-specific protein-tyrosine kinase	S157	−1.86	0.0042	5 weeks
563	P05412	Jun	Jun proto-oncogene-encoded AP1 transcription factor	Pan-specific	−1.41	0.0054	5 weeks
553	P45983	JNK1/2/3	Jun N-terminus protein-serine kinases (stress-activated protein kinase (SAPK)) 1/2/3	Pan-specific	−1.85	0.0062	5 weeks
133	P55212	CASP6	Pro-caspase 6 (apoptotic protease Mch2)	Pan-specific	−1.43	0.0075	5 weeks
915	Q05655	PKCδ	Protein-serine kinase C delta	Pan-specific	−1.49	0.0097	5 weeks
667	P45985	MEK4	MAPK/ERK protein-serine kinase 4 (MKK4)	S257 + T261	−1.55	0.0114	2 weeks
211	P78368	CK1g2	Casein protein-serine kinase 1 gamma 2	Pan-specific	−1.53	0.0222	5 weeks
555	P45983	JNK	Jun N-terminus protein-serine kinase (stress-activated protein kinase (SAPK))	T183/Y185	−1.21	0.0242	5 weeks
607	P07948	Lyn	Yes-related protein-tyrosine kinase	Pan-specific	−1.51	0.0271	5 weeks
1181	P12931	Src	Src proto-oncogene-encoded protein-tyrosine kinase	Y529	1.26	0.0451	5 weeks
137	Q14790	CASP8	Pro-caspase 8 (ICE-like apoptotic protease 5 (ICE-LAP5), Mch5, FLICE, CAP4)	Pan-specific	−1.45	0.0457	5 weeks
779	Q16539	p38a MAPK	Mitogen-activated protein-serine kinase p38 alpha	Pan-specific	1.37	0.0478	5 weeks
881	P31749	PKBa (Akt1)	Protein-serine kinase B alpha	T308	1.43	0.0485	5 weeks
317	P27361	Erk1	Extracellular regulated protein-serine kinase 1 (p44 MAP kinase)	T202 + Y204; T185/Y187	1.32	0.0489	5 weeks

in ventral spinal horn below the level of transection, allow us to hypothesize that inhibition of cap-dependent protein translation plays a significant role in sub-acute phase after spinal cord trauma and might contribute to the healing process in the damaged region. The key roles of angiogenesis and neurodegeneration pathways are highlighted together with direct cross-talk mediated by several hub proteins belonging to the family of proteins with Src homology-2 domains such as Lck and Lyn kinases or SHP2 with the phosphorylation site for PKC [50]. The attenuated capacity of angiogenesis after SCI, which was described previously [51,52] may be due to decreased expression of receptors such as TEK/TIE2, FGFR and IGFR but not vascular endothelial growth factor receptor (VEGFR) observed in our study. In addition, the regulation of down-stream effector components of angiogenesis may even have a greater effect in preventing angiogenesis failure. Such scenario is exemplified by up-regulation of HSP27 and MAPK3/ERK1 activating phosphorylation.

To pursue any beneficial targeting of specific proteins, we focused on proteins that appear to have important relevance in the development of spasticity state and may potentially serve as new targets in developing new pharmacological or gene silencing/up-regulation-based treatment strategies.

PKCδ is the isoform of PKC protein family belonging to the class of novel PKCs which are regulated by diacylglycerol but not calcium. In our study, PKCδ was constitutively expressed in subpopulation of α-motoneurons and interneurons and in APC positive glial cells. At 5 weeks after transection a significant increase in PKCδ was measured (Fig. 4) and this increase was primarily seen in microglial cells throughout the gray and white matter. Previous experimental data showed that increased PKCδ activity in spinal parenchyma could be involved in potentiating spinal neuronal excitability [53]. It has been demonstrated that PKCδ mediates IL-6-induced nociceptive responses in inflammatory and tumor-induced pain models in mice [54]. Injury severity-dependent increase in spinal parenchymal IL-6 was previously demonstrated [55]. Thus a similar mechanism involving IL-6/PKCδ-mediated increase in α-motoneuron responsiveness to peripheral stimuli may be present in spinal trauma-induced spasticity. Using the model of murine microglial cells, it was shown [56] that knockdown of PKCδ attenuated selectively ERK1/2 phosphorylation, blocked NF-κB activation and suppressed inducible nitric oxide synthase (iNOS) in reactive microglia. Selective spinal blockade of NOS by intrathecal delivery of L-NAME (a non-selective NOS inhibitor) lead to a potent suppression of Ia-afferent mediated H-reflex [57] and this effect was likely mediated through the suppression of L-NAME-sensitive NMDA receptor-coupled secondary glutamate release [58]. We speculate that an increase in iNOS/eNOS activity in reactive microglial cells initiated in part by increased PKCδ level/

Author's personal copy

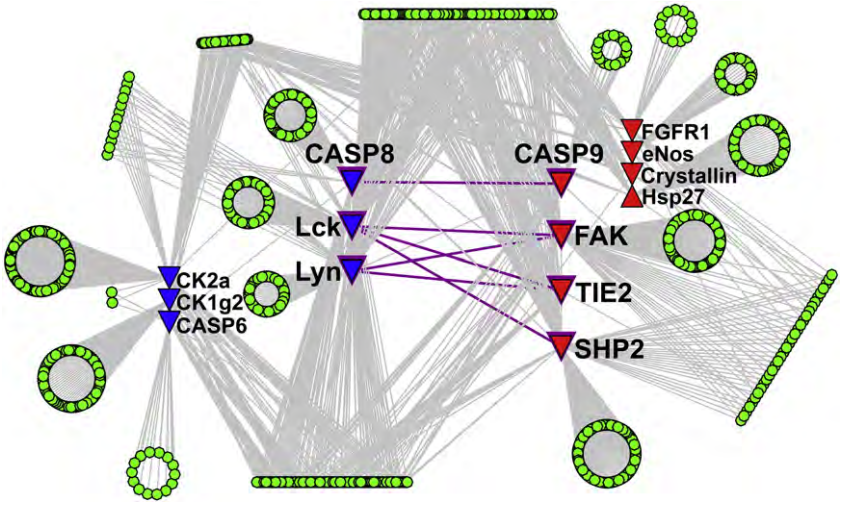

Fig. 3 – Protein–protein interaction network connecting signaling proteins of angiogenesis and neurodegeneration during evolving spasticity after spinal Th9 transection. Computer modeling of protein–protein interactions depicts a high number of mediated interactions among selected proteins assigned by PANTHER database to angiogenesis (red) or neurodegeneration (blue) and highlights direct interconnections among several key proteins indicated by violet. The network generated by NAVIGaTOR software is best interpreted as follows: nodes represent proteins and edges between nodes represent physical interactions between proteins. The trends of protein changes are shown by triangles.

activity may play a key role in the potentiation of neuronal activity through its NMDA-receptor-coupled facilitatory effect on neurons residing in previously trauma injured segments. Additionally, activation of bradykinin presynaptic and postsynaptic B(2) receptors, has been demonstrated to potentiate synaptic glutamate release and contribute to spinal central sensitization which is attenuated by PKC inhibition [59].

The phosphorylation of MAPK3/ERK1 which enables kinase activation was also significantly increased in spinal parenchyma at 5 weeks after spinal transection. Previous studies have shown that spinal up-regulation and activation of MAPK/ERK contribute to inflammatory pain after peripheral nerve injury [60] and are overexpressed in spinal trauma-injured segments, which correspond to the presence of mechanical allodynia [61]. Intrathecal treatment with ERK inhibitor reverses mechanical allodynia in L5 spinal nerve ligation model [62] and normalizes mechanical and heat stimulation response threshold in upper cervical spinal nerve transection model in rat [63]. The mechanism through which the MAPKs exert their stimulatory neuronal effect is complex and involves regulation of the activity of glutamate receptors, potassium channels and transcriptional induction of several genes [23]. Accordingly, and as for RONα (see below), we hypothesize that activation of spinal parenchymal MAPKs including ERK1 through their effector systems can lead to facilitatory effect of primary afferents and/or direct activation of ventral α-motoneurons.

The high level of CaMKIV was one of the most significant changes which preceded the onset of spasticity. This protein belongs to the Ca^{2+}/calmodulin family of Ser/Thr protein kinases known as CaMKs and is known to be a distinct second

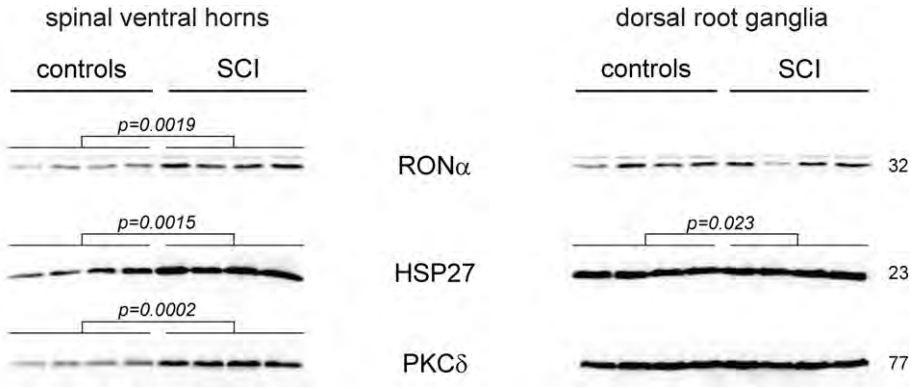

Fig. 4 – Verification of RONα, HSP27 and PKCδ protein levels in ventral horns and dorsal root ganglia cells in rats after Th9 spinal transection using western blot analysis. The immunoblot experiments were performed to verify changes in the levels of RONα, HSP27, and PKCδ. The results of the analysis shown confirmed significantly higher level of RONα and HSP27 in dorsal ventral horns 5 weeks after spinal injury. Contrarily to decrease in PKCδ level observed on microarray, western blot showed significant increase of this protein in ventral horns 5 weeks after transection.

Author's personal copy

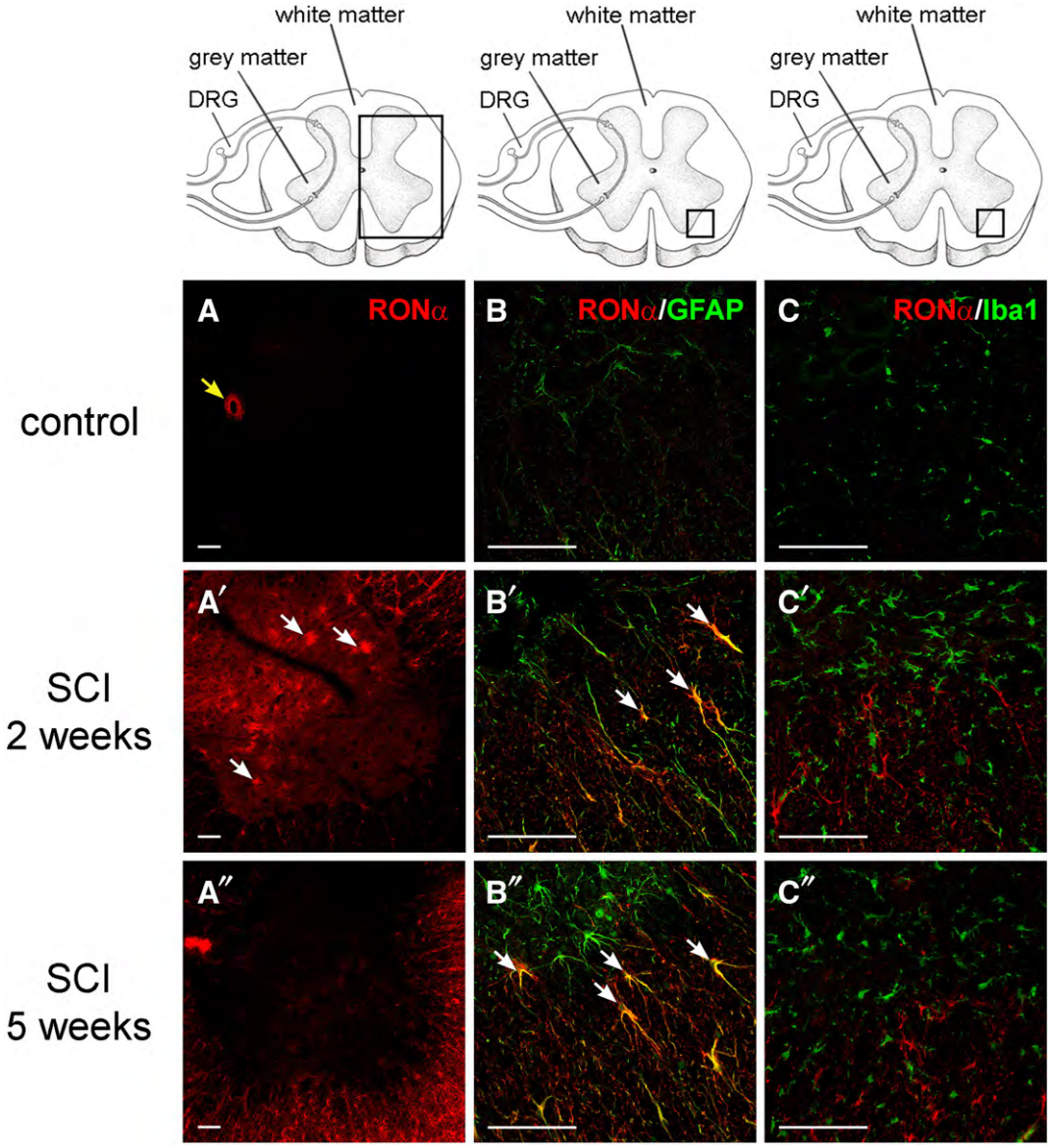

Fig. 5 – Immunofluorescence examination of the presence of RONα-expressing cell in spinal (L3–4) parenchyma in naïve-control animals and in animals at 2 or 5 weeks after Th9 spinal transection. (A, B, C) In naïve animals, staining with RONα antibody showed relatively weak immunoreactivity in ependymal cells of central canal (A; yellow arrow). No RONα expression in GFAP+ astrocytes or Iba1+ microglial cells was seen (B, C). (A′, B′, C′) In contrast to control, an intense RONα expression in α-motoneurons and interneurons was seen at 2 weeks after spinal transections (A′; white arrows). In addition, numerous double-labeled RONα/GFAP+ astrocytes localized on the border of gray and white matter were identified (B′; white arrows). No co-localization of RONα expression with microglial marker (Iba1) was seen (C′). (A″, B″, C″) At 5 weeks after spinal transections, the RONα expression in neuronal populations was near completely lost (A″) but continued to be present in activated GFAP+ astrocytes (B″; white arrowheads) but not in microglial cells (C″). Scale bars: 100 μm.

messenger and potent stimulator of Ca^{2+}-dependent gene expression [64]. Previous studies have demonstrated an important role of the CaMKII in modulation of synaptic plasticity via phosphorylation of neuronal membrane receptors [65], and also in long-term potentiation (LTP) and early synaptic LTP in the anterior cingulate cortex in mice [66]. While the role of CaMKIV in exacerbated neuronal activation under different pathological states has not been sufficiently studied, another member of this protein family, CaMKII, has been directly linked to several pathways associated with the development of chronic pain states resulting from peripheral nerve or spinal cord injury. One example demonstrating this, is the intradermal injection of capsaicin associated with increased expression and phosphorylation of CaMKII in rat spinal dorsal horn neurons. In the same study the nociceptive behavior resulting from capsaicin injection was effectively blocked by spinal CaMKII inhibition [67]. While a direct link between the activity of CaMKII and the effector system which mediate nociceptive responses on cellular-neuronal level is not fully understood, several postulated mechanisms have been proposed including: i) the cyclic

Author's personal copy

adenosine CREB is up-regulated after spinal trauma in spinal segments which corresponds to permanent mechanical allodynia [61]; ii) the CaMKII inhibitor (AIP)-mediated anti-nociceptive effect is associated with decreased spinal parenchymal CREB activity in the rat chronic peripheral nerve injury model [68]; and iii) and activated CaMKII enhances phosphorylation of neuronal AMPA receptor GluR1 subunits after peripheral nociceptive stimulus [67]. Jointly, these data indicate that the activation of CaMKII can lead to up-regulation of postsynaptic AMPA GluR1 receptor through Ca^{2+}-dependent CREB activation. Such a neuronal AMPA GluR1 overexpression can then lead to increased responsiveness of affected neurons to local or peripheral-input driven excitatory drive. In keeping with this hypothesis, our previous data showed a significant increase in α-motoneuron GluR1 expression in animals with chronic spinal ischemia-induced spasticity and a potent anti-spasticity effect after systemic or intrathecal treatment with AMPA receptor antagonist (NGX 424) [19,20]. Interestingly, compared to CaMKII, CaMKIV is localized in nucleus where it may directly phosphorylate/activate proinflammatory proteins, mainly CREB [69].

RONα is receptor tyrosine kinase of Met proto-oncogene family and specific receptor for macrophage-stimulating protein (MSP). Our current data showed an intense RONα expression in neuronal and glial populations at 2 weeks after spinal transections and continuing presence of RONα in activated astrocytes at 5 weeks after transection. Previous studies have shown that zymosan-induced inflammation of L5 DRGs neurons in rat is associated with prolonged mechanical hyperalgesia and together with other cytokines such as IL-5 and IL-10, leads to an increased MSP in previously inflamed DRGs [70]. The primary source from which the MSP is being released and can activate RON-expressing neurons can be multifactorial and may include MSP-synthesizing local activated microglia, astrocytes or neurons [71,72]. Alternatively, the circulating MSP from the blood stream can be the source of MSP in spinal areas with trauma-induced blood–brain barrier disruption [73]. Accordingly, we speculate that a robust expression of RONα in spinal α-motoneurons at 2 weeks after injury may play a significant role in the initiation of spasticity response during the same time frame. In addition, the fact that not only α-motoneurons but also interneuronal populations overexpressed RONα, indicates that these classes of excitatory interneurons can similarly be responsive to a local MSP stimulation and may directly facilitate primary afferent activity and/or trigger α-motoneuron depolarization through activation of glutamate classes of receptors.

Interestingly, none of the proteins found to be up-regulated in spinal parenchyma were increased in DRG extracts. These findings show that in the absence of any direct primary afferent activation (whether mechanical, thermal of inflammation-triggered) the DRGs are quite inert to a centrally-mediated trauma, particularly if the trauma site is relatively distant from the primary afferent innervating below injury-intact segments. These findings also indicate that the development of tactile-mechanical hypersensitivity and muscle stretch-evoked spasticity is primarily related to the loss of local spinal parenchymal-segmental inhibition and/or facilitatory effect of local inflammatory processes on primary afferent activity. Hence, resultant potential new treatment strategies such as gene silencing or drug treatment should primarily target spinal parenchymal sites at and around the injury epicenter and will likely employ intrathecal or targeted spinal segment-specific vector or drug delivery.

5. Conclusion

In the present study by using a well established Th9 spinal transection model of muscle spasticity, we characterized protein changes at 2 or 5 weeks after spinal transection in spinal ventral horn and DRG extracts from spinal segment below the level of transection. The eIF4G Ser1107 hyperphosphorylation and pronounced decreases in protein levels in ventral spinal horn as well as direct protein interaction mediated cross-talk between angiogenesis and neurodegeneration pathways were highlighted and might significantly contribute to healing process in the damaged region. Several proteins including CaMKIV, RONα, MAPK3/ERK1 and PKCδ were found to be significantly up-regulated/activated in spinal parenchyma but not in corresponding DRGs. These results indicate that the activities of these signaling molecules may not only play an important role in the initiation but also in the maintenance of spasticity states after spinal trauma. The exclusivity of specific protein changes to lumbar spinal parenchyma but not to DRGs also indicates that new treatment strategies (whether pharmacological or gene-based therapies) should primarily target dermatome-muscle-specific spinal segments to improve local inhibitory tone and/or decrease the primary afferent drive in prevention of spasticity development or treatment of spasticity states.

Conflict of interest

There are no conflicts of interest to report. No writing assistance was utilized in the production of this manuscript.

Acknowledgment

This work was supported in part by MEYS (ME10044; H.K.), NIH (NS051644; M.M.), TACR (TA01011466; HK), and Institutional Research Concept RVO67985904 (IAPG, AS CR, v.v.i). Infrastructural part of this project was supported from the Operational Program Research and Development for Innovations (CZ.1.05/2.1.00/03.0124).

Appendix A. Supplementary data

Supplementary data to this article can be found online at http://dx.doi.org/10.1016/j.jprot.2013.06.028.

REFERENCES

[1] Lance JW. Spasticity: disordered motor control. In: Feldman RG, Young RR, Koella WP, editors. Symposium synopsis. Chicago: Year Book Medical Publishers; 1980. p. 485–94.
[2] Maurice V, Allan HR, Raymond DA. Adams & Victor's principles of neurology. 7th ed. McGraw-Hill Companies; 2001 .

Author's personal copy

[3] Thuret S, Moon LD, Gage FH. Therapeutic interventions after spinal cord injury. Nat Rev Neurosci 2006;7:628–43.
[4] Elbasiouny SM, Moroz D, Bakr MM, Mushahwar VK. Management of spasticity after spinal cord injury: current techniques and future directions. Neurorehabil Neural Repair 2010;24:23–33.
[5] Nielsen JB, Crone C, Hultborn H. The spinal pathophysiology of spasticity—from a basic science point of view. Acta Physiol (Oxf) 2007;189:171–80.
[6] Noreau L, Proulx P, Gagnon L, Drolet M, Laramee MT. Secondary impairments after spinal cord injury: a population-based study. Am J Phys Med Rehabil 2000;79:526–35.
[7] Boulenguez P, Liabeuf S, Bos R, Bras H, Jean-Xavier C, Brocard C, et al. Down-regulation of the potassium-chloride cotransporter KCC2 contributes to spasticity after spinal cord injury. Nat Med 2010;16:302–7.
[8] Li Y, Gorassini MA, Bennett DJ. Role of persistent sodium and calcium currents in motoneuron firing and spasticity in chronic spinal rats. J Neurophysiol 2004;91:767–83.
[9] Marsala M, Hefferan MP, Kakinohana O, Nakamura S, Marsala J, Tomori Z. Measurement of peripheral muscle resistance in rats with chronic ischemia-induced paraplegia or morphine-induced rigidity using a semi-automated computer-controlled muscle resistance meter. J Neurotrauma 2005;22:1348–61.
[10] Siddall P, Xu CL, Cousins M. Allodynia following traumatic spinal cord injury in the rat. Neuroreport 1995;6:1241–4.
[11] Eide PK, Stubhaug A, Stenehjem AE. Central dysesthesia pain after traumatic spinal cord injury is dependent on N-methyl-D-aspartate receptor activation. Neurosurgery 1995;37:1080–7.
[12] Katz R. Presynaptic inhibition in humans: a comparison between normal and spastic patients. J Physiol Paris 1999;93:379–85.
[13] Mazzocchio R, Rossi A. Involvement of spinal recurrent inhibition in spasticity. Further insight into the regulation of Renshaw cell activity. Brain 1997;120(Pt 6):991–1003.
[14] Boorman GI, Lee RG, Becker WJ, Windhorst UR. Impaired "natural reciprocal inhibition" in patients with spasticity due to incomplete spinal cord injury. Electroencephalogr Clin Neurophysiol 1996;101:84–92.
[15] Remy-Neris O, Barbeau H, Daniel O, Boiteau F, Bussel B. Effects of intrathecal clonidine injection on spinal reflexes and human locomotion in incomplete paraplegic subjects. Exp Brain Res 1999;129:433–40.
[16] Krach LE. Pharmacotherapy of spasticity: oral medications and intrathecal baclofen. J Child Neurol 2001;16:31–6.
[17] Kamen L, Henney 3rd HR, Runyan JD. A practical overview of tizanidine use for spasticity secondary to multiple sclerosis, stroke, and spinal cord injury. Curr Med Res Opin 2008;24:425–39.
[18] ElBasiouny SM, Schuster JE, Heckman CJ. Persistent inward currents in spinal motoneurons: important for normal function but potentially harmful after spinal cord injury and in amyotrophic lateral sclerosis. Clin Neurophysiol 2010;121:1669–79.
[19] Hefferan MP, Kucharova K, Kinjo K, Kakinohana O, Sekerkova G, Nakamura S, et al. Spinal astrocyte glutamate receptor 1 overexpression after ischemic insult facilitates behavioral signs of spasticity and rigidity. J Neurosci 2007;27:11179–91.
[20] Oshiro M, Hefferan MP, Kakinohana O, Lukacova N, Sugahara K, Yaksh TL, et al. Suppression of stretch reflex activity after spinal or systemic treatment with AMPA receptor antagonist NGX424 in rats with developed baclofen tolerance. Br J Pharmacol 2010;161:976–85.
[21] Gao YJ, Ji RR. Chemokines, neuronal–glial interactions, and central processing of neuropathic pain. Pharmacol Ther 2010;126:56–68.
[22] Cruz CD, Cruz F. The ERK 1 and 2 pathway in the nervous system: from basic aspects to possible clinical applications in pain and visceral dysfunction. Curr Neuropharmacol 2007;5:244–52.
[23] Ji RR, RWt Gereau, Malcangio M, Strichartz GR. MAP kinase and pain. Brain Res Rev 2009;60:135–48.
[24] Wang Y, Wu J, Lin Q, Nauta H, Yue Y, Fang L. Effects of general anesthetics on visceral pain transmission in the spinal cord. Mol Pain 2008;4:50.
[25] Willis WD. Role of neurotransmitters in sensitization of pain responses. Ann N Y Acad Sci 2001;933:142–56.
[26] Aimone JB, Leasure JL, Perreau VM, Thallmair M. Spatial and temporal gene expression profiling of the contused rat spinal cord. Exp Neurol 2004;189:204–21.
[27] Bareyre FM, Schwab ME. Inflammation, degeneration and regeneration in the injured spinal cord: insights from DNA microarrays. Trends Neurosci 2003;26:555–63.
[28] Ding Q, Wu Z, Guo Y, Zhao C, Jia Y, Kong F, et al. Proteome analysis of up-regulated proteins in the rat spinal cord induced by transection injury. Proteomics 2006;6:505–18.
[29] Chen A, McEwen ML, Sun S, Ravikumar R, Springer JE. Proteomic and phosphoproteomic analyses of the soluble fraction following acute spinal cord contusion in rats. J Neurotrauma 2010;27:263–74.
[30] Kang SK, So HH, Moon YS, Kim CH. Proteomic analysis of injured spinal cord tissue proteins using 2-DE and MALDI-TOF MS. Proteomics 2006;6:2797–812.
[31] Kunz S, Tegeder I, Coste O, Marian C, Pfenninger A, Corvey C, et al. Comparative proteomic analysis of the rat spinal cord in inflammatory and neuropathic pain models. Neurosci Lett 2005;381:289–93.
[32] Yan X, Liu J, Luo Z, Ding Q, Mao X, Yan M, et al. Proteomic profiling of proteins in rat spinal cord induced by contusion injury. Neurochem Int 2010;56:971–83.
[33] Mann M, Ong SE, Gronborg M, Steen H, Jensen ON, Pandey A. Analysis of protein phosphorylation using mass spectrometry: deciphering the phosphoproteome. Trends Biotechnol 2002;20:261–8.
[34] Pelech S, Jelinkova L, Susor A, Zhang H, Shi X, Pavlok A, et al. Antibody microarray analyses of signal transduction protein expression and phosphorylation during porcine oocyte maturation. J Proteome Res 2008;7:2860–71.
[35] Pelech S, Zhang H. Plasticity of the kinomes in monkey and rat tissues. Sci STKE 2002;2002:pe50.
[36] Skalnikova H, Vodicka P, Pelech S, Motlik J, Gadher SJ, Kovarova H. Protein signaling pathways in differentiation of neural stem cells. Proteomics 2008;8:4547–59.
[37] Thomas PD, Campbell MJ, Kejariwal A, Mi H, Karlak B, Daverman R, et al. PANTHER: a library of protein families and subfamilies indexed by function. Genome Res 2003;13:2129–41.
[38] Brown KR, Jurisica I. Online predicted human interaction database. Bioinformatics 2005;21:2076–82.
[39] Zhang H, Pelech S. Using protein microarrays to study phosphorylation-mediated signal transduction. Semin Cell Dev Biol 2012;23:872–82.
[40] Nakao-Hayashi J, Ito H, Kanayasu T, Morita I, Murota S. Stimulatory effects of insulin and insulin-like growth factor I on migration and tube formation by vascular endothelial cells. Atherosclerosis 1992;92:141–9.
[41] Wang MH, Zhou YQ, Chen YQ. Macrophage-stimulating protein and RON receptor tyrosine kinase: potential regulators of macrophage inflammatory activities. Scand J Immunol 2002;56:545–53.
[42] Lance JW. The control of muscle tone, reflexes, and movement: Robert Wartenberg Lecture. Neurology 1980;30:1303–13.
[43] Barolat G, Myklebust JB, Wenninger W. Effects of spinal cord stimulation on spasticity and spasms secondary to myelopathy. Appl Neurophysiol 1988;51:29–44.
[44] Arroyo R, Vila C, Clissold S. Retrospective observational study of the management of multiple sclerosis patients with resistant spasticity in Spain: the '5E' study. Expert Rev Pharmacoecon Outcomes Res 2011;11:205–13.

Author's personal copy

[45] Ashworth NL, Satkunam LE, Deforge D. Treatment for spasticity in amyotrophic lateral sclerosis/motor neuron disease. Cochrane Database Syst Rev 2006:CD004156.
[46] Botte MJ, Nickel VL, Akeson WH. Spasticity and contracture. Physiologic aspects of formation. Clin Orthop 1988:7–18.
[47] Dabney KW, Lipton GE, Miller F. Cerebral palsy. Curr Opin Pediatr 1997;9:81–8.
[48] Abbott R, Forem SL, Johann M. Selective posterior rhizotomy for the treatment of spasticity: a review. Childs Nerv Syst 1989;5:337–46.
[49] Barolat G. Surgical management of spasticity and spasms in spinal cord injury: an overview. J Am Paraplegia Soc 1988;11: 9–13.
[50] Strack V, Krutzfeldt J, Kellerer M, Ullrich A, Lammers R, Haring HU. The Protein-tyrosine-phosphatase SHP2 is phosphorylated on serine residues 576 and 591 by protein kinase C isoforms alpha, beta 1, beta 2, and eta. Biochemistry 2002;41:603–8.
[51] Beattie MS, Bresnahan JC, Komon J, Tovar CA, Van Meter M, Anderson DK, et al. Endogenous repair after spinal cord contusion injuries in the rat. Exp Neurol 1997;148:453–63.
[52] Kawabe J, Koda M, Hashimoto M, Fujiyoshi T, Furuya T, Endo T, et al. Neuroprotective effects of granulocyte colony-stimulating factor and relationship to promotion of angiogenesis after spinal cord injury in rats: laboratory investigation. J Neurosurg Spine 2011;15:414–21.
[53] Esper RM, Loeb JA. Neurotrophins induce neuregulin release through protein kinase Cdelta activation. J Biol Chem 2009;284:26251–60.
[54] Andratsch M, Mair N, Constantin CE, Scherbakov N, Benetti C, Quarta S, et al. A key role for gp130 expressed on peripheral sensory nerves in pathological pain. J Neurosci 2009;29: 13473–83.
[55] Yang L, Jones NR, Blumbergs PC, Van Den Heuvel C, Moore EJ, Manavis J, et al. Severity-dependent expression of pro-inflammatory cytokines in traumatic spinal cord injury in the rat. J Clin Neurosci 2005;12:276–84.
[56] Wen J, Ribeiro R, Zhang Y. Specific PKC isoforms regulate LPS-stimulated iNOS induction in murine microglial cells. J Neuroinflammation 2011;8:38.
[57] Tasci N, Ankarali S, Demir S. Further evidence for enhancing effects of NO on monosynaptic and polysynaptic spinal reflexes in cats. Brain Res 2003;980:109–16.
[58] Sorkin LS. NMDA evokes an L-NAME sensitive spinal release of glutamate and citrulline. Neuroreport 1993;4:479–82.
[59] Kohno T, Wang H, Amaya F, Brenner GJ, Cheng JK, Ji RR, et al. Bradykinin enhances AMPA and NMDA receptor activity in spinal cord dorsal horn neurons by activating multiple kinases to produce pain hypersensitivity. J Neurosci 2008;28:4533–40.
[60] Zhuang ZY, Gerner P, Woolf CJ, Ji RR. ERK is sequentially activated in neurons, microglia, and astrocytes by spinal nerve ligation and contributes to mechanical allodynia in this neuropathic pain model. Pain 2005;114:149–59.
[61] Crown ED, Ye Z, Johnson KM, Xu GY, McAdoo DJ, Hulsebosch CE. Increases in the activated forms of ERK 1/2, p38 MAPK, and CREB are correlated with the expression of at-level mechanical allodynia following spinal cord injury. Exp Neurol 2006;199:397–407.
[62] Obata K, Yamanaka H, Kobayashi K, Dai Y, Mizushima T, Katsura H, et al. Role of mitogen-activated protein kinase activation in injured and intact primary afferent neurons for mechanical and heat hypersensitivity after spinal nerve ligation. J Neurosci 2004;24:10211–22.
[63] Kobayashi A, Shinoda M, Sessle BJ, Honda K, Imamura Y, Hitomi S, et al. Mechanisms involved in extraterritorial facial pain following cervical spinal nerve injury in rats. Mol Pain 2011;7:12.
[64] Anderson KA, Noeldner PK, Reece K, Wadzinski BE, Means AR. Regulation and function of the calcium/calmodulin-dependent protein kinase IV/protein serine/threonine phosphatase 2A signaling complex. J Biol Chem 2004;279:31708–16.
[65] Wayman GA, Lee YS, Tokumitsu H, Silva AJ, Soderling TR. Calmodulin-kinases: modulators of neuronal development and plasticity. Neuron 2008;59:914–31.
[66] Toyoda H, Zhao MG, Mercaldo V, Chen T, Descalzi G, Kida S, et al. Calcium/calmodulin-dependent kinase IV contributes to translation-dependent early synaptic potentiation in the anterior cingulate cortex of adult mice. Mol Brain 2010;3:27.
[67] Fang L, Wu J, Lin Q, Willis WD. Calcium-calmodulin-dependent protein kinase II contributes to spinal cord central sensitization. J Neurosci 2002;22: 4196–204.
[68] Wang Y, Cheng X, Xu J, Liu Z, Wan Y, Ma D. Anti-hyperalgesic effect of CaMKII inhibitor is associated with downregulation of phosphorylated CREB in rat spinal cord. J Anesth 2011;25: 87–92.
[69] Wayman GA, Tokumitsu H, Davare MA, Soderling TR. Analysis of CaM-kinase signaling in cells. Cell Calcium 2011;50:1–8.
[70] Xie WR, Deng H, Li H, Bowen TL, Strong JA, Zhang JM. Robust increase of cutaneous sensitivity, cytokine production and sympathetic sprouting in rats with localized inflammatory irritation of the spinal ganglia. Neuroscience 2006;142:809–22.
[71] Shafit-Zagardo B, Sharma N, Berman JW, Bornstein MB, Brosnan CF. CSF-1 expression is upregulated in astrocyte cultures by IL-1 and TNF and affects microglial proliferation and morphology in organotypic cultures. Int J Dev Neurosci 1993;11:189–98.
[72] Takeuchi A, Miyaishi O, Kiuchi K, Isobe K. Macrophage colony-stimulating factor is expressed in neuron and microglia after focal brain injury. J Neurosci Res 2001;65:38–44.
[73] Franzen R, Bouhy D, Schoenen J. Nervous system injury: focus on the inflammatory cytokine 'granulocyte-macrophage colony stimulating factor'. Neurosci Lett 2004;361:76–8.